Desalination and Water Treatment

Ultrafiltration of oil/water emulsions using PVDF/PC blend membranes

Martin A. Masuelli [a]

[a] Instituto de Física Aplicada, CONICET , Universidad Nacional de San Luis , Chacabuco 917
(ZC: 5700), San Luis , Argentina Phone: Tel./Fax: +54 2652 432068
Published online: 07 Oct 2013.

PLEASE SCROLL DOWN FOR ARTICLE

Ultrafiltration of oil/water emulsions using PVDF/PC blend membranes

Martin A. Masuelli

Instituto de Física Aplicada, CONICET, Universidad Nacional de San Luis, Chacabuco 917 (ZC: 5700), San Luis, Argentina
Tel./Fax: +54 2652 432068; email: masuelli@unsl.edu.ar

ABSTRACT

Membranes with varying degrees of hydrophilicity made from blends of poly(vinylidene fluoride) (PVDF) and polycarbonate (PC) were prepared to recover water from emulsified oily wastewater. The effects of different amounts of PC content on the structure, hydrophilicity, and functionality of these PVDF/PC membranes were analyzed using contact angle measurements, scanning electron microscope and energy dispersion X-ray analysis, liquid–liquid displacement, and a fouling test with an oil/water emulsion. The slightly hydrophilic character of the PC decreases the hydrophobicity of the blend membranes compared to a pure PVDF membrane. Increasing the amount of PC in the casting solution causes little change in average pore size but a substantial change in the membrane's porosity and surface structure, with these changes reflected in the efficiency of the membranes with respect to recovering water from the emulsified oily wastewater. The best performance, meaning less membrane fouling and better permeate quality, was obtained using a blend membrane containing 20% PC, which achieved an initial permeate flux of $28.59 \, \text{L/m}^2 \, \text{h}$ with a limiting permeate flux of $22.11 \, \text{L/m}^2 \, \text{h}$, a COD of 88 ppm in the permeate solution, and 97.8% oil retention.

Keywords: Poly(vinylidene fluoride); Polycarbonate; Blend membranes; Oily wastewater emulsion; Ultrafiltration

1. Introduction

Membrane separation is a unit operation applied in the chemical, food, pharmaceutical, and biotechnology industries as well as in effluent treatment technology. Membrane filtration processes are used in industry for conventional separation and offer potential advantages such as highly selective separation, separation of some secondary materials, and operation at room temperature. There are usually no phase changes involved, and operations can be continuous and automated with low costs. The application of membrane processes holds a special interest where certain types of materials must be separated, such as fine dispersions, colloidal particles, biological materials, and emulsions. Emulsions produced in the metal-working industry have a potential for causing environmental damage and these pollutants must therefore be reduced by treatment. In order to perform separation using a membrane process, the first step is to develop a membrane suitable for the physical and chemical properties of the substances to be filtered.

Ultrafiltration (UF) processes suffer flux decline over time, in some cases down to a fraction of the flux for pure water. This is due to processes that are both reversible and irreversible, such as concentration polarization near the membrane surface, fouling caused by adsorption of solutes, plugging of membrane pores. Furthermore, gel layer formation due to solubility limits and the presence of suspended particles can exacerbate these flux reductions. In UF of oil/water emulsions, reversible and irreversible adsorption of emulsion drops is considered to be the main fouling mechanism, and these adsorbed emulsion drops cannot be easily removed by washing with anion surfactant solutions or with water [1]. Studies of fouling by colloidal materials such as natural organic matter and polysaccharides have been performed by Płatkowska-Siwiec and Bodzek [2] and Shi et al. [3], who obtained encouraging results regarding the processes involved in membrane fouling.

Hydrophobic polymers such as polysulfone, polypropylene, and poly(vinylidene fluoride) (PVDF) are widely used as membrane materials because of their good chemical resistance and superior thermal and mechanical properties [4]. However, a membrane with an affinity for organic compounds in the feed solution can readily cause fouling in these hydrophobic materials. Several means are therefore commonly employed in order to minimize fouling, including modification of operational parameters during the UF processes and efforts focused on the membrane material itself. Numerous efforts to modify membrane materials to make them less susceptible to fouling have been reported in the literature, and blending of the original polymer with other polymers having more suitable properties has been one approach examined [5].

Poly(vinylidene fluoride) (PVDF) is a polymer widely used for producing porous membranes for a variety of biomedical applications, UF technologies, etc. PVDF membranes are usually prepared by immersion of a cast solution in a polymer non-solvent bath [6,7]. The properties of PVDF membranes in relation to structure, porosity, flux, and retention are controlled by varying the casting and immersion parameters [8–10]. Chemical or plasma treatment and grafting or graft polymerizations are also widely used techniques for membrane surface modification, in order to decrease a membrane's hydrophobic character with consequent variation of its binding properties [11,12].

Blend membranes have now emerged as new technologies for oily wastewater treatment [13–15]. Fouling studies with oil emulsions have been performed using microporous PVDF membranes, with easy removal of the particles deposited achieved by successive washings at low trans-membrane pressures

[16]. PVDF blend membranes have also been hydrophilized with PES by UV irradiation, producing membranes with low BSA absorption [17]. Composite PVDF membranes with Al_2O_3 and TiO_2 have been used for UF of an oil emulsion, with such membranes possessing low-fouling properties [18].

A method to prepare PVDF–polyhedral oligomeric silsesquioxane (POSS) systems has also been developed, characterized by silsesquioxane molecules grafted onto the polymer surface. This approach consists of a preliminary modification of the PVDF by chemical treatment with an alkaline solution in order to obtain unsaturations, then a subsequent surface reaction of the PVDF modified with POSS molecules characterized by an amino group as the reactive side [19].

Grafting between a methoxy poly(ethylene glycol) (MPEG) and hyperbranched polyester (HPE) has produced an amphiphilic polymer hyperbranched-star (HPE–g–MPEG). This can be mixed with PVDF to form a blend with little change in the contact angle compared to pure PVDF. Furthermore, these blend membranes showed lower protein static adsorption, higher water and protein solution fluxes, and better water flux recovery after cleaning than the pure PVDF membrane [20]. A PVDF blend membrane with cellulose acetate propionate (CAP) was prepared by the phase inversion process, and this membrane showed a lower reduction in porosity with a flow of pure water compared to the membrane without CAP [21]. Studies on the creation of a PVDF/polycarbonate (PC) blend using PMMA as a compatibilizer have demonstrated that the use of 40% PMMA generates an increase in miscibility and a beneficial effect on the mechanical properties of the resulting membranes [22–24].

In the work reported here, PVDF and PC blend membranes for use in UF applications were prepared using a non-solvent induced phase inversion technique. These synthesized membranes were studied using scanning electron microscope (SEM) microscopy and were characterized by their contact angle (θ), average pore size by liquid–liquid displacement porosimetry (LLDP), and hydraulic permeability. Fouling tests were performed using an oil/water emulsion, with the effluent quality analyzed in terms of chemical oxygen demand (COD) and oil content rejection ($R_{oil}\%$). A resistances model was created to describe the phenomenon of membrane fouling.

2. Experimental approach

2.1. Materials

High-viscosity Solef® 1,015 PVDF was obtained from Solvay Belgium and 85 kDa polyvinylpyrrolidone

(PVP) was obtained from Stanton (Argentina). *N,N*-dimethylacetamide (DMAc) was obtained from Merck, and Lexan PC was purchased from General Electric and used as provided. Viledon 2431 non-woven support (thickness: 0.14 mm; air permeability at 200 Pa: 500 L/m²h) was provided by Carl Freudenberg, Germany.

Commercial oil (Insignia® oil) was purchased from JyM Lubricantes. (Argentina). An oil/water emulsion was prepared by mixing 1 g of Insignia® oil in 1 L of distilled water (0.1% w/v oil concentration) by stirring with an UltraTurrax-T50 stirrer at 500 rpm. The emulsion had the following characteristics: pH 7, viscosity $\eta = 1.058 \times 10^{-3}$ Pa s, COD 1,700 mg L^{-1}, and average oil droplet diameter 2.5 μm, measured with a Carl Zeiss Pol II microscope [25].

2.2. Membrane preparation

The general procedure used for membrane preparation was as follows: 15% w/v of PVDF and 2% w/v of PVP were dissolved in DMAc at 50°C by stirring with a magnetic bar for 10 h. Next, different amounts of PC (5, 10, and 20% w/w with respect to PVDF) were added and dissolved. The final mixture was cast onto the non-woven support (FO2430, Freudenberg) at 25°C using a film extensor. The supported polymeric film solution was then coagulated in bi-distilled water at 25°C. Finally, the membrane was placed in a 5 L water bath for 12 h. Higher PC concentrations (i.e. 25–30% w/w) were found to produce a water flux-tight composite membrane.

In order to evaluate the hydrophilic/hydrophobic characteristics of the PC material, a dense membrane was synthesized from a 5% w/w solution of PC in dichloromethane. The polymer solution was cast onto a flat glass, and the dense membrane was obtained after solvent evaporation at 298 K.

2.3. Contact angle measurement

The hydrophobic character of the PVDF/PC blend membranes was determined by measuring the water-membrane contact angle (θ) using the sessile-drop technique and a contact angle device (Micromeritics Instrument Corporation, Norcross, GA, USA). The contact angle value was measured 3 min after dropping water on the membrane surface, and three drops of water were measured for each membrane sample. The average contact angles (θ) with a standard deviation of ±2 were determined using the following expression [26]:

$$\cos\theta = 1 - \sqrt{\frac{Bh^2}{\left(1 - \frac{Bh^2}{2}\right)}} \tag{1}$$

$$B = \frac{\rho g}{2\gamma} \tag{2}$$

with g being gravity acceleration (980 cm/s²), ρ the density of bi-distilled water (0.9971 g/cm³), γ the interfacial tension of bi-distilled water (71.97 erg/cm²), and h the height of the liquid drop.

2.4. SEM and energy dispersion X-ray (EDX) measurements

The morphologies of the blend membranes were observed using a LEO 1450VP SEM, with EDX analysis performed with a Genesis 2000 at an acceleration voltage of 120 kV. For the morphological analysis, cross-section samples were prepared by fracturing the membranes after immersion in liquid nitrogen and coating with carbon.

2.5. Pore size and porosity measurements by LLDP

A three-liquid mixture of isobutanol/methanol/water (15/7/25 by vol., surface tension $\gamma = 0.35$ mN/m) was used analyze the pores by applying relatively low pressures [14]. The procedure used consists of filling the membrane with a liquid (wetting liquid, aqueous phase) and then displacing it from the pores with the organic phase (isobutanol saturated with water and methanol). Flux through the membrane was obtained by using a syringe pump (Isco 500D) to gradually increase the flux on the organic-phase side. Simultaneously, equilibrium pressure is measured at each incremental stage using a pressure transducer (OMEGA DP200). By monitoring the applied pressure and the flux through the membrane, the radii of the opened pores at each applied pressure can be calculated using Cantor's equation. This equation is valid if it is assumed that the liquid effectively wets the membrane (i.e. with null contact angle).

$$r_P = \frac{2\gamma}{\Delta p} \tag{3}$$

where Δp = applied pressure, γ = interfacial tension, and r_P = equivalent pore radius. Assuming cylindrical pores, the Hagen–Poiseuille relationship can then be used to correlate volumetric flux density J_{vi} to a given pore radius r_P. For each incremental stage of volumetric flux density, the corresponding pressure (Δp_i) was measured. From these data, the distribution of the

number of pores (n_i) vs. pore radius was calculated according to:

$$\frac{dn_i}{dr_{pi}} = -\frac{\eta\tau\ell\Delta p_i^6}{16\pi\gamma^6}\frac{d^2J_{vi}}{d\Delta p_i^2} \tag{4}$$

where η = dynamic viscosity, τ = tortuosity, and ℓ = pore length, which corresponds to the active layer thickness of the membrane, $\ell = 0.75\,\mu m$ is obtained from SEM image. A value accepted by several authors [27,28] to the tortuosity is 1.4, since its measurement is very difficult to perform correctly.

The membrane surface porosity (ε) can be then calculated using [29]:

$$\varepsilon = \frac{\pi n r_p^2}{A_m} \tag{5}$$

where A_m is the membrane surface area ($2.46 \times 10^{-3}\,m^2$), and n is pores number.

2.6. Hydraulic permeability and fouling tests

Fig. 1 presents a schematic diagram of the complete retentate recycling, lab-scale UF device used in this study. The polymeric membrane was placed in the permeation cell with a transfer area of $A = 3 \times 10^{-3}\,m^2$. The pure water or oil–water emulsion was pumped through the top side of the membrane surface using a peristaltic pump (Masterflex), with 7,000 s of fouling operation. The operating conditions in terms of hydraulic permeability measurements (L_H), feed flow rate ($v = 1\,L/min$), and temperature

Fig. 1. UF device: (1) feed solution reservoir (Haake 1C), (2) peristaltic pump, (3) pressure gauge, (4) permeation cell (Minitan S), (5) membrane, (6) needle valve, (7) flowmeter, (8) retentate, (9) permeate, (10) analytical balance (Ohaus explorer), and (11) data acquisition system.

($T = 25°C$) were kept constant, while the trans-membrane pressure Δp was varied from 50 to 80 kPa. The oil emulsion flux experiments were performed at $v = 1\,L/min$, $T = 25°C$, and $\Delta p = 67\,kPa$. These maximum values for feed velocity and pressure used in the experimental runs were constrained by the operational capacity of the pump. The recycled retentate flow was measured with a flowmeter and the permeate flux was determined by time weighing the permeate solution; with an analytical balance interfaced with a computer used to collect and process the mass data for permeate vs. time.

In order to analyze the fouling phenomena, membranes were cleaned *in situ* after the emulsion UF testing using the following protocol: an anionic surfactant (sodium dodecilsulfate) was pumped through the membrane surface for 30 min, and then, the membrane was washed with pure water for 30 min. After each cleaning procedure, the hydraulic permeability of the treated membranes (L_{HC}) was evaluated at $T = 25°C$.

2.7. Chemical oxygen demand (COD)

COD measurements were performed by placing the samples under reflux in a strongly acidic solution with a predetermined excess of potassium dichromate. Consumed oxygen was measured against standards at 600 nm using a Hitachi U-2001 UV–vis spectrophotometer (standard methods for the examination of water and wastewater 5220D).

2.8. Oil content

Oil content was evaluated by UV–vis spectroscopy (wavelength of 220 nm) using the calibration curve obtained from oil pattern solutions. Oil content rejection ($R_{oil}\%$) was evaluated using the following equation:

$$R_{oil}\% = 100\frac{c_{oil,F} - c_{oil,P}}{c_{oil,F}} \tag{6}$$

where $c_{oil,F}$ and $c_{oil,P}$ are the oil/water concentrations in the feed and permeate, respectively.

3. Results and discussion

3.1. Structural and chemical characteristics of the membrane

The micrographs seen in Figs. 2(b) and 3 show that the PC significantly affects the membrane's porosity and surface structure, while the PVDF membrane can be seen in Fig. 2(a) and (c) to have a finger-like porous structure [30]. Backscattered electron images allow observation of phase changes in a given material, as
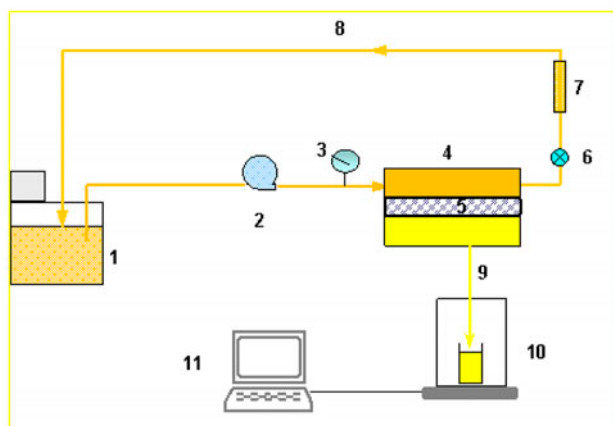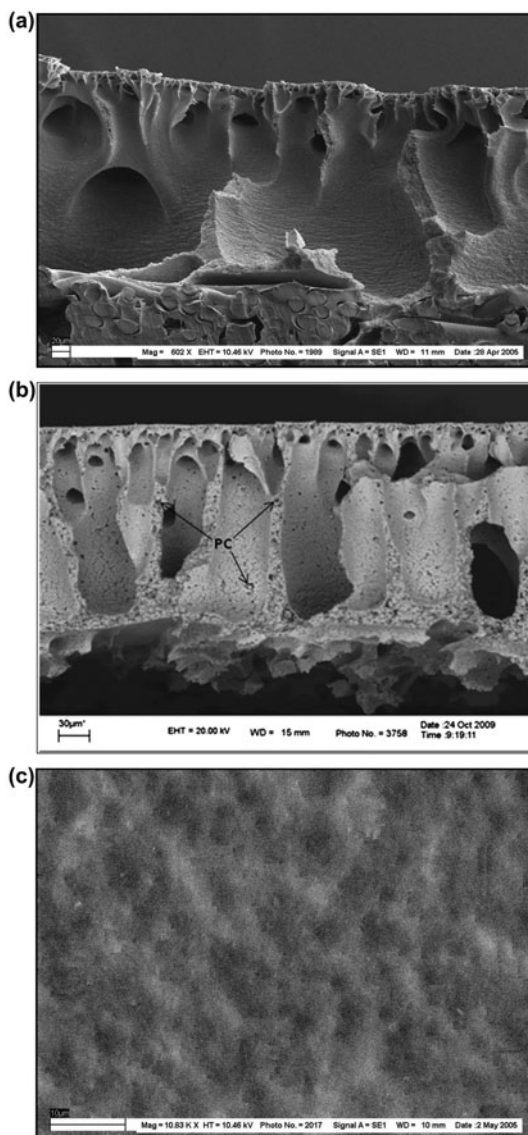
Fig. 2. SEM images (a) cross-section of 15PVDF membrane at 602X; (b) cross-section of 15PVDF20PC membrane at 700X, and (c) upper surface of 15PVDF membrane at 10.83KX.

Fig. 3. Backscattered-electron SEM micrograph and EDX of 15PVDF20PC membrane, 10KX magnification: (a) PC; (b) PC/PVDF, and (c) PVDF.

seen here in Fig. 3. By using this technique, small PC spheres and cylinders can be seen in the PVDF matrix, indicating a heterogeneous blend of the PC and PVDF and demonstrating that compatibility between these polymers is not high. PC can be observed as inserted into the PVDF with structures from 0.5 to 1.0 μm in all of the transversal sections and surface images. These structures observed for PC/PVDF, such as in Fig. 3(b), do not reveal any sort of clear boundary between the two polymers.

The poor compatibility seen between PC/PVDF reflects the fact that the phase inversion process was
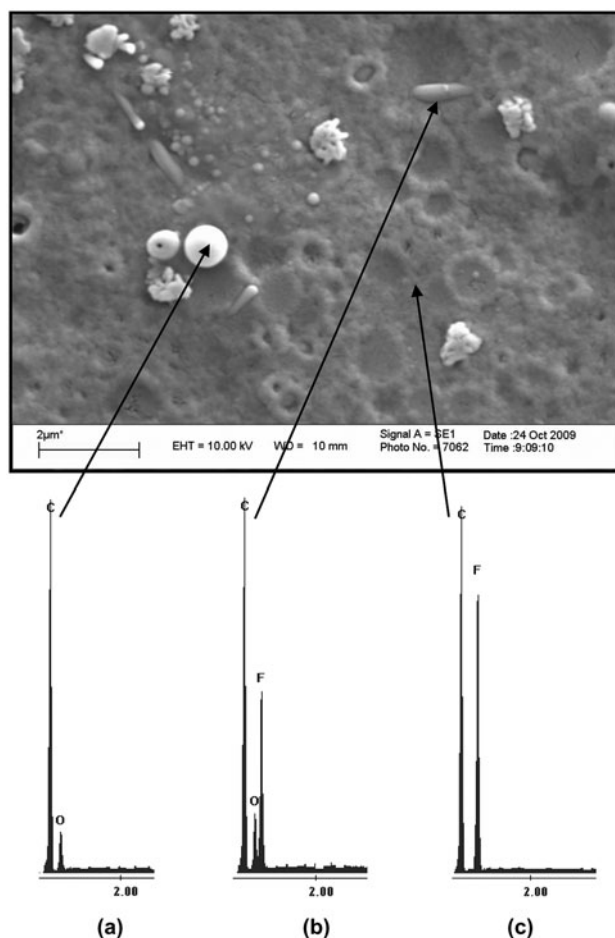
performed at 50℃ for the polymer solution while the coagulation bath was 25℃, and therefore, the rate of solvent–nonsolvent exchange should be slow to reach thermodynamic equilibrium. This ultimately produces a less dense, compact layer with slightly smaller pores, whereas the porous substructure acquires a finger-like shape. A similar decrease in pore size was observed by Awanis Hashim et al. [31], where reduction of pore size ranged from 2.38 to 2.08 nm in poly (ether sulfone) membranes prepared by the phase inversion process with polymer solution temperatures of 25−90℃. Kim et al. [32] reported an increase in the poly(ether imide) membrane dense layer when changing the ratio of solvent and co-solvent in coagulation at 70℃, with structural changes seen between the porous substructure and the dense layer.

In terms of the influence of coagulation temperature, polymer concentration, and cast film thickness on the membrane morphology, when the polymer

concentration in the casting dope increases, the membranes obtained by coagulation under the same conditions show a morphology with a denser spongious phase and fewer macrovoids. Such a change in membrane morphology is expected, since a more concentrated polymer solution leads to a higher polymer concentration in the system at the bi-nodal phase separation point (hence a denser spongious structure), as well as a reduced possibility of solvent extraction from the surrounding polymer solution to the polymer-lean phase during formation of the macrovoids. The pore structure of the skin formed on the face in contact with water would also change in the same way, that is, porosity and the pore size would decrease with increasing polymer concentration in the casting dope. When the PVDF/PC is blended with the original PVDF, the morphology of the coagulated membranes is different than that of single polymer membranes: irregular macrovoids, and eventually polymer nodules, instead of finger-like macrovoids. These would be generated by compressive strains that appear in the skin layer bonded to a soft substrate (liquid polymer dope) during the departure of the solvent from the nascent membrane toward the coagulation bath. A decrease either in coagulation temperature or in the total polymer in the casting dope led to larger and more numerous macrovoids, probably due to an increase in the phase separation time before gelling of the system [33].

The SEM imaging results were complemented by EDX measurements. Fig. 3 shows the SEM surface image of the 15PVDF20PC membrane with the EDX spectra for dark, bright, and intermediate zones. Small spheres and agglomerates from 0.5 to 1.0 μm can be observed in the images as inserted into the PVDF upper surface. The SEM-EDX analysis of the 15PVDF20PC membrane shows that the sphere on the surface of the membrane (bright zone, Fig. 3(a)) corresponds to pure PC ($C = 8$ 8.4% and $O = 11.6\%$), the intermediate zone (Fig. 3(b)) indicates a PC/PVDF blend agglomerate ($C = 60.4\%$, $O = 9.6\%$, and $F = 30\%$), and the dark zone (Fig. 3(c)) corresponds to pure

PVDF ($C = 57.3\%$ and $F = 42.7\%$). This demonstrates that the polymeric blend of PC and PVDF was heterogeneous and indicates a low affinity between the two polymeric materials [22–24].

3.2. Hydrophobic character and mean pore radius of the membranes

Table 1 shows the membrane contact angles, mean pore radius, hydraulic permeabilities, COD, and $R_{oil}\%$ with their standard deviations. The contact angle values for PC ($60 < \theta < 70$) reflect its slightly hydrophilic character, related to the dipole–dipole and induced dipole–dipole contributions. The hydrophobic character of PVDF ($\theta > 80$) is related to the van der Waals interactions and that of the PC/PVDF blend membranes is related to the contributions of the hydroxyl and fluor groups.

Pore size distributions for the membranes ranged between 27.31 and 31.88 nm (Table 1 and Fig. 4), with a considerable population of pores having a radius larger than r_P. It can be seen that there is a decrease in average pore radius for the membranes with PC. This phenomenon can be explained by the phase inversion process, where a solvent–nonsolvent exchange results in a loss of stability for the polymer in the casting solution, with PC particles trapped in the polymer matrix. During the phase inversion process, the entry of non-solvent generates interfacial defects between the PC phase and polymer phase leading to a slight decrease in r_P.

3.3. Emulsion permeability and fouling

Water flux values (J_v) at different Δp were used to evaluate water permeability (L_H) by use of Darcy's law as follows:

$$L_H = \frac{J}{\Delta p} = \frac{1}{\eta R_m} \tag{7}$$

Table 1
Structural and functional characteristics of the synthesized membranes

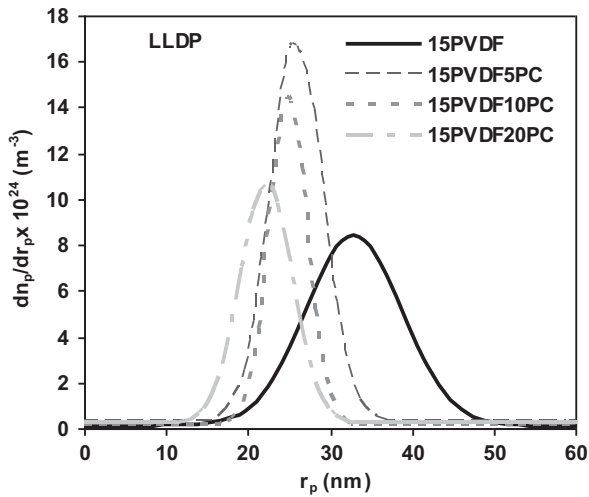| Membrane	θ	r_P (nm)	ε	J_{vo} (L/m²h)	L_{HI} (L/m² kPa h)	L_{HC} (L/m² kPa h)	COD ppm O₂	$R_{oil}\%$
15PVDF	80 ± 3.6	31.88 ± 1.3	0.70 ± 0.11	72.36 ± 5.6	1.064 ± 0.144	0.283 ± 0.023	214 ± 2.12	86.5 ± 1.12
15PVDF5PC	76 ± 3.3	29.21 ± 2.1	0.53 ± 0.15	57.45 ± 6.8	0.836 ± 0.124	0.265 ± 0.014	167 ± 1.99	89.0 ± 1.44
15PVDF10PC	74 ± 2.9	28.45 ± 2.5	0.47 ± 0.14	35.54 ± 7.9	0.522 ± 0.121	0.234 ± 0.011	135 ± 1.87	93.6 ± 1.89
15PVDF20PC	71 ± 3.1	27.31 ± 1.7	0.35 ± 0.12	28.59 ± 5.7	0.433 ± 0.075	0.223 ± 0.012	88 ± 1.55	97.8 ± 1.53
PC	68 ± 2.2	–	–	–	–	–	–	–

Fig. 4. Pore size distribution for the synthesized membranes.

where R_m is the intrinsic membrane resistance and η is solvent viscosity.

From Table 1, it can be observed that the L_{HC} values for all of the membranes were similar ($L_{HC} = 0.283–0.223$ L/h m^2 kPa), with a 73.41% decrease in hydraulic permeability for the 15PVDF membrane compared to its initial value ($L_{HI} = 1.0645$ L/h m^2 kPa), but with only a 48.59% decrease for the 15PVDF20PC membrane. This suggests that after the cleaning procedure the surfaces and/or the porous structures of all of the membranes were modified, with the modified membranes showing little difference in the L_{HC} values, as seen in table 1.

Oil separation efficiency was determined for the membranes by their retention coefficient (Eq. (6)), while the hydraulic permeability test was performed by comparing hydraulic permeability values after fouling and cleaning with a water-SDS solution (L_{HC}) to the initial hydraulic permeability (L_{HI}) values. The data seen in Table 1 clearly indicate a decrease in initial hydraulic permeability paralleling an increase in PC content. This phenomenon may be explained by considering that increasing PC levels in the polymeric casting solution led to a decrease in porosity in the dense layer. This L_{HI} decrease, from 1.0645 to 0.4338 (L/m^2 kPa h), may also be related to the more uniform pore size distribution seen in the PC membranes. The data plotted for L_{HC} are similar up to 10% PC, with the lowest value seen in the 20% PC membrane. This 15PVDF20PC membrane shows a recovery of the initial permeate flow in its L_{HC} value after washing with SDS.

The blend membranes have excellent properties for water recovery. The membranes with PC showed lower θ values, along with a decrease in r_p [15]. This is due to the low porosity of the PC membranes, which can be explained qualitatively from SEM images showing the low affinity of PVDF/PC. The most interesting point observed after fouling (permeate flow drop in Fig. 5) is that the L_{HI} is partially recovered with the 15PVDF20PC membrane after washing.

The measured porosities (ε) as determined by the LLDP method are also shown in Table 1. As can be seen, the membranes with PC all show L_H y ε values lower than those of the 15PVDF membrane [14,15].

Fig. 6 shows the normalized flow decline with the oil/water emulsion for the prepared membranes. The most marked flow decline is seen in the membrane with no PC and therefore the highest fouling. As the PC content increases in the membrane, this reduction in flux decreases, with the lowest amount seen in the 15PVDF20PC membrane.
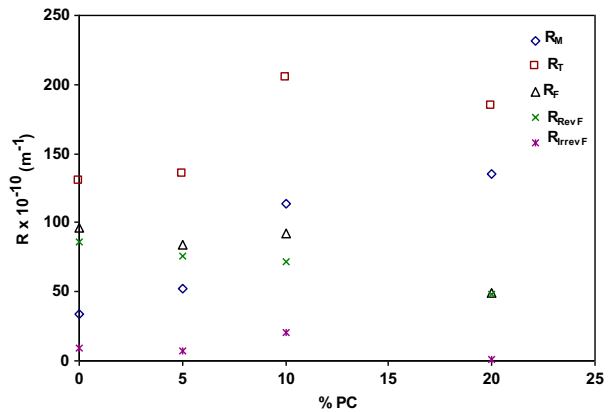

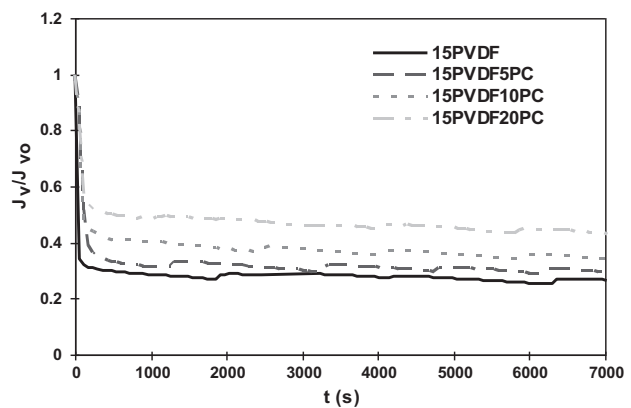Fig. 5. Membrane resistances as a function of PC/PVDF content.

Fig. 6. J_v/J_{vo} vs. time for the synthesized membranes.

Mass permeate flux during filtration can be expressed in terms of a resistance model as follows:

$$J_v = \frac{dV}{Adt} = \frac{\Delta p}{\eta(R_M + R_F)} \qquad (8)$$

where J_V is the permeate flux ($m^3/m^2 s$), Δp the applied pressure (Pa), R_T the total resistance of permeation (m^{-1}), and η (Pa s) the permeate viscosity. R_T includes the membrane's intrinsic resistance (R_M) and the fouling resistance (R_F), or $R_T = R_M + R_F$. The osmotic effect, the effect of polarization by concentration, and the effect of fouling are all included in R_F, which is in turn subdivided into reversible fouling (R_{RevF}) and irreversible fouling (R_{IrrevF}).

$$R_F = R_{RevF} + R_{IrrevF} \qquad (9)$$

To determine the values of R_{IrrevF} and R_{RevF}, we proceeded to wash with aqueous solution of SDS (30 min), then washed with water (30 min) and from the extent of flux density (J_v) was calculated the resistance reversible fouling and subtracting this value to the fouling resistance (R_F) is calculated irreversible fouling resistance.

The resistance model data are shown in Fig. 5. The blend membranes present less fouling compared to the PVDF membranes. The PVDF membranes present reversible and irreversible fouling, while those with 5% PC content ($\theta = 68$) can markedly reduce irreversible fouling. As θ decreases, the value of L_{HI} decreases for the 15PVDF10PC and 15PVDF20PC membranes, fouling resistance is lowered and irreversible fouling is reduced. Only a small decrease in permeate flux occurs in these membranes [34–36]. This decrease is diminished by washing with a flux of pure water, thus removing particles that are weakly adhered to pores and to the membrane surface.

Washes with SDS (L_{HC}) did not allow recovery of the initial permeability (L_{HI}), suggesting that the irreversible fouling is well adsorbed, and this procedure has difficulty in removing the emulsion droplets on the surface and in the pores of the membrane. This phenomenon is due to an increase in the membrane's hydrophilicity and does not result in a reduction of irreversible fouling. The interaction between the membrane and the emulsion during fouling generates a strong deposition of emulsion droplets on the surface and in the pores of the membrane. Washing with water easily removes the more weakly adsorbed emulsion droplets but it does not remove the more strongly adsorbed. However, washing with SDS produced enough interaction to remove the strongly adsorbed emulsion droplets, which is manifested in the L_{HC} values.

The PVDF/PC blend membranes prepared show increased hydrophilicity with increasing PC content, although they do not fully recover their initial levels of permeate flow after fouling. In spite of this, PVDF membranes containing 10 and 20% PC have high oil content rejection ($R_{oil}\%$) and COD values of less than 100 ppm O_2. This means that the permeate quality falls within Argentina's existing water quality regulations for surface irrigation [37].

4. Conclusions

Blend membranes were prepared using the wet phase inversion process, by adding increasing amounts of PC to a PVDF casting solution. This blending process allowed production of PVDF/PC membranes with a hydrophilic character, while also producing a new pore structure due to phase separation. The results of this study indicate that PVDF and PC are not very compatible, and that the interface microvoid produced therefore results from the shallow phase separation in PVDF/PC. The hydrophilicity of PVDF/PC membranes is evidently improved by increasing the PC in the blends, as demonstrated by decreasing contact angles and hydraulic permeability measurements. However, increasing the PC content in the blend membranes resulted in similar mean pore radius measurements (r_p of 27.31−31.88 nm). This trend is attributed to the finger-like pores becoming larger and the skin layer becoming more compact with increasing PC content. Moreover, PC can result in improved low-fouling properties for PVDF/PC membranes [9,38,39]. The contact angle is affected by aspects of the surface morphology such as surface roughness and membrane pore size. There is currently no experimental method to measure hydrophilicity as a unique property of a membrane's chemistry [40]. Increasing PC content generated a decrease in the hydraulic permeability of these membranes and a slight decrease in mean pore radius. The 15PVDF20PC membrane has a low stain resistance and low irreversible fouling, with its permeate COD being below the limit established by law in Argentina [37], or in other words less than 100 ppm O_2. Oil content rejection for the membranes containing PC was higher than 86.50% in all cases.

Acknowledgements

Symbols

B	—	constant measure of contact angle
G	—	acceleration of gravity
H	—	height of the liquid
J_V	—	permeate flux
J_{vi}	—	volumetric flux density
L	—	pore longitude
n_k	—	pore numbers
$\Delta p, \Delta p$	—	applied pressure
Q_i	—	distribution of pore radius by LLDP
R_F	—	fouling resistance
R_{IrrevF}	—	irreversible fouling
R_M	—	membrane resistance
$R_{oil}\%$	—	oil content rejection percent
r_P	—	pore equivalent radium
r_P	—	porous radius by LLDP
R_{RevF}	—	reversible fouling
R_T	—	total resistance of permeation

Greek

γ	—	interfacial tension
η	—	dynamic viscosity
θ	—	contact angle
ρ	—	liquid density
τ	—	pore tortuosity

References

[1] P. Ramesh Babu, V.G. Gaikar, Membrane characteristics as determinant in fouling of UF membranes, Sep. Purif. Technol. 24 (2001) 23–34.

[2] A. Płatkowska-Siwiec, M. Bodzek, The influence of membrane and water properties on fouling during ultrafiltration, Desal. Wat. Treat. 35 (2011) 235–241.

[3] X. Shi, R. Field, N. Hankins, Review of fouling by mixed feeds in membrane filtration applied to water purification, Desalin. Water Treat. 35 (2011) 68–81.

[4] F. Liu, N.A. Hashim, Y. Liu, M.R. Abed, K. Li, Progress in the production and modification of PVDF membranes, J. Membr. Sci. 375 (2011) 1–27.

[5] A. Bottino, G. Capannelli, A. Comite, Novel porous membranes from chemically modified poly(vinylidene fluoride), J. Membr. Sci. 273 (2006) 20–24.

[6] T.-H. Young, L.-W. Chen, Pore formation mechanism of membranes from phase inversion process, Desalination 103 (1995) 233–247.

[7] D.-J. Lin, C.-L. Chang, F.-M. Huang, L.-P. Cheng, Effect of salt additive on the formation of microporous poly(vinylidene fluoride) membranes by phase inversion from LiClO4/ Water/DMF/PVDF system, Polymer 44 (2003) 413–422.

[8] X. Tan, S.P. Tan, W.K. Teo, K. Li, Polyvinylidene fluoride (PVDF) hollow fibre membranes for ammonia removal from water, J. Membr. Sci. 271 (2006) 59–68.

[9] E. Fontananova, J.C. Jansen, A. Cristiano, E. Curcio, E. Drioli, Effect of additives in the casting solution on the formation of PVDF membranes, Desalination 192 (2006) 190–197.

[10] J.-H. Kim, K.-H. Lee, Effect of PEG additive on membrane formation by phase inversion, J. Membr. Sci. 138 (1998) 153–163.

[11] D.M. Brawls, I. Mathieson, I. Sutherland, R.A. Cayless, R.H. Dahm, Pretreatment of poly(vinyl fluoride) and poly(vinylidene fluoride) with potassium hydroxide, Int. J. Adhes. Adhes. 16 (1996) 87–95.

[12] G. Botelho, M.M. Silva, A.M. Gonçalves, V. Sencadas, J. Serrado-Nunes, S. Lanceros-Mendez, Performance of electroactive poly(vinylidene fluoride) against UV radiation, Polym. Testing 27 (2008) 818–822.

[13] Y.W. Kim, D.K. Lee, K.J. Lee, J.H. Kim, Single-step synthesis of proton conducting poly(vinylidene fluoride) (PVDF) graft copolymer electrolytes, Eur. Polym. J. 44 (2008) 932–939.

[14] N.A. Ochoa, M. Masuelli, J. Marchese, Effect of hydrophilicity on fouling of an emulsified oil wastewater with PVDF/ PMMA membranes, J. Membr. Sci. 226 (2003) 203–211.

[15] M. Masuelli, J. Marchese, N.A. Ochoa, SPC/PVDF membranes for emulsified oily wastewater treatment, J. Membr. Sci. 326 (2009) 688–693.

[16] Y. Wang, X. Chen, J. Zhang, J. Yin, H. Wang, Investigation of microfiltration for treatment of emulsified oily wastewater from the processing of petroleum products, Desalination 249 (2009) 1223–1227.

[17] M. Zhang, Q.T. Nguyen, Z. Ping, Hydrophilic modification of poly (vinylidene fluoride) microporous membrane, J. Membr. Sci. 327 (2009) 78–86.

[18] Q. Zhao, H. Lu, S. Yu, Study on oilfield wastewater treatment with composite nanoparticles modified PVDF UF membrane, in: K. Starkey (Ed.), 5th International Conference on Bioinformatics and Biomedical Engineering, ICBBE 2011, Berlin, Global Community Technology, art. N° 5780984, ISSN 978-1-4244-5089-3/11/2011 IEEE.

[19] O. Monticelli, P. Waghmare, A. Chincarini, On the preparation and application of novel PVDF–POSS systems, J. Mater. Sci. 44 (2009) 1764–1771.

[20] Y.-H. Zhao, B.-K. Zhu, L. Kong, Y.-Y. Xu, Improving hydrophilicity and protein resistance of poly(vinylidene fluoride) membranes by blending with amphiphilic hyperbranched-star polymer, Langmuir 23 (2007) 5779–5786.

[21] Hui-Hsin Tseng, Guo-Liang Zhuang, S. Yun-Chieh, The effect of blending ratio on the compatibility, morphology, thermal behavior and pure water permeation of asymmetric CAP/PVDF membranes, Desalination 284 (2012) 269–278.

[22] N. Moussaif, P. Marechal, R. Jerome, Ability of PMMA to improve the PC/PVDF interfacial adhesion, Macromolecules 30 (1997) 658–659.

[23] N. Moussaif, C. Pagnoulle, R. Jerome, Reactive compatibilization of PC/PVDF polymer blends by zinc carboxylate containing poly(methylmethacrylate) ionomers, Polymer 41 (2000) 5551–5562.

[24] N. Moussaif, R. Jerome, Compatibilization of immiscible polymer blends (PC/PVDF) by the addition of a third polymer (PMMA): Analysis of phase morphology and mechanical properties, Polymer 40 (1999) 3919–3932.

[25] N.A. Ochoa, M. Masuelli, J. Marchese, Development of charged ion exchange resin-polymer ultrafiltration membranes to reduce organic fouling, J. Membr. Sci. 278 (2006) 457–463.

[26] J.I. Calvo, A. Bottino, G. Capannelli, A. Hernández, Comparison of liquid–liquid displacement porosimetry and scanning electron microscopy image analysis to characterize ultrafiltration track-etched membranes, J. Membr. Sci. 239 (2004) 189–197.

[27] M.H.V. Mulder, Basic Principles of Membrane Technology, Kluiwer Academic, Dordrecht, 1991.

[28] F.P. Cuperus, C.A. Smolders, Characterization of UF membranes, membrane characteristics and characterization techniques, Adv. Colloid Interface Sci. 34 (1991) 135–173.

[29] S.J. Gregg, K.S.W. Sing, Adsorption, Surface Area and Porosity, 2nd ed., Academic Press, New York, NY, 1992.

[30] M.A. Masuelli, M. Grasselli, J. Marchese, N.A. Ochoa, Preparation, structural and functional characterization of modified porous PVDF membranes by γ-irradiation, J. Membr. Sci. 389 (2012) 91–98.

[31] N. Awanis Hashim, F. Liu, K. Li, A simplified method for preparation of hydrophilic PVDF membranes from an amphiphilic graft copolymer, J. Membr. Sci. 345 (2009) 134–141.

[32] Y. Kim, D. Rana, T. Matsuuraa, W.-J. Chung, K.C. Khulbe, Relationship between surface structure and separation performance of poly(ether sulfone) ultra-filtration membranes blended with surface modifying macromolecules, Sep. Purif. Technol. 72 (2010) 123–132.

[33] J. Zhou, J. Ren, L. Lin, M. Deng, Morphology evolution of thickness-gradient membranes prepared by wet phase-inversion process, Sep. Purif. Technol. 63 (2008) 484–486.

[34] J.-F. Blanco, J. Sublet, Q.T. Nguyen, P. Schaetzel, Formation and morphology studies of different polysulfones-based membranes made by wet phase inversion process, J. Membr. Sci. 283 (2006) 27–37.

[35] M. Zhang, Q.T. Nguyen, Z. Ping, Hydrophilic modification of poly (vinylidene fluoride) microporous membrane, J. Membr. Sci. 327 (2009) 78–86.

[36] D. Wang, K. Li, W.K. Teo, Preparation and characterization of polyvinylidene fluoride (PVDF) hollow fiber membranes, J. Membr. Sci. 163 (1999) 211–220.

[37] Ley Nacional de Residuos Peligrosos (Hazardous Residue National Law). N° 24051. Available from: http://www.infoleg.mecon.gov.ar/infolegInternet/verNorma.do?id=450.

[38] N. Li, C. Xiao, S. An, X. Hu, Preparation and properties of PVDF/PVA hollow fiber membranes, Desalination 250 (2010) 530–537.

[39] M.G. Buonomenna, L.C. Lopez, P. Favia, R. d'Agostino, A. Gordano, E. Drioli, New PVDF membranes: The effect of plasma surface modification on retention in nanofiltration of aqueous solution containing organic compounds, Water Res. 41 (2007) 4309–4316.

[40] D. Rana, T. Matsuura, Surface modifications for antifouling membranes, Chem. Rev. 110 (2010) 2448–2471.